Capacity and Capacity Sensitivity of Soft Output Optical Channels

Jon Hamkins, Samuel Dolinar, Dariush Divsalar, Fabrizio Pollara

Jet Propulsion Laboratory, California Institute of Technology
4800 Oak Grove Dr., Pasadena, CA 91109-8099

ABSTRACT

In this paper we derive the capacity of Pulse Position Modulation (PPM).on a general soft output, memoryless channel, and evaluate the capacity formula for a variety of optical channel models, including AWGN, Webb [1], and Webb plus Gaussian distributions. Unlike a typical RF link, the optical channel has correlated signal and noise, complicating the statistical model to the point that capacity and code performance cannot be summarized by a single SNR parameter. Nevertheless, we are able to define a small set of fundamental parameters (two for AWGN and three for Webb) which are sufficient to determine the capacity. Numerical results indicate that over a wide range of operating points, a single fundamental parameter dominates the capacity calculation.

A second contribution of the paper is the description of the relationship between the fundamental parameters and a multitude of physical parameters that describe the laser, channel, and detector. Using this relationship and the gradient of capacity, the sensitivity of capacity with respect to each fundamental and physical parameter is derived. This enables engineers to focus laser and detector development efforts in areas that will result in the largest capacity increases.

Keywords: Capacity, pulse position modulation, avalanche photodiode detector, Webb statistics, sensitivity

1. INTRODUCTION

The problem of determining the capacity of Pulse Position Modulation (PPM) on a soft output channel is motivated by the deep-space optical channel. NASA has considerable interest and hope in this channel as a means to deliver data to Earth faster, more reliably, and with less energy expended. Recent research at the Jet Propulsion Laboratory has led to the consideration of optical communications systems that use a Q-switched laser, Pulse Position Modulation (PPM), and an Avalanche PhotoDiode (APD) detector, and it is important that we be able to define the ultimate performance capability of this type of channel to provide a foundation on which mission designers can build.

We consider the communication system shown in Fig. 1. A k-bit source $\mathbf{U} = (U_1, \ldots, U_k) \in \{0,1\}^k$ is modulated with $(M = 2^k)$-ary PPM to yield a signal $\mathbf{X} = (0, \ldots, 0, 1, 0, \ldots, 0) \in \{0,1\}^M$, which contains a single one in the position indicated by the binary representation of $\mathbf{U}$. The transmission channel is a binary-input unconstrained-output memoryless channel. One use of the overall PPM-symbol channel consists of M serial uses of the binary-input channel, and produces the received vector $\mathbf{Y} = (Y_1, \ldots Y_M) \in \mathbb{R}^M$. This vector is then sent through an invertible transformation $Y_j \to V_j, 1 \leq j \leq M$, to produce $\mathbf{V} = (V_1, \ldots V_M) \in \mathbb{R}^M$. The conditional probability density function (pdf) of V_i given $X_i = 0$ or 1 is denoted by $p_0(\cdot)$ or $p_1(\cdot)$, respectively.

2. CAPACITY OF SOFT OUTPUT PPM

The capacity of the system in Fig. 1 is given by the maximum mutual information between V and $\mathbf{U}$:

$$C = \max_{p(\mathbf{U})} I(\mathbf{V}; \mathbf{U}) = \max_{p(\mathbf{X})} I(\mathbf{V}; \mathbf{X}) \text{ bits per channel use,}$$

where the second equality follows because $\mathbf{X}$ is an invertible function of $\mathbf{U}$. By "channel use" we mean one use of the PPM-symbol channel. The PPM modulator can be viewed as an encoder producing the $M = 2^k$ codewords

The work described was funded by the TMOD **Technology Program and performed by the Jet Propulsion Laboratory, California Institute of Technology under contract with the National Aeronautics and Space Administration.**
Email: {jon.hamkins, samuel.dolinar, dariush.divsalar, fabrizio.pollara}@jpl.nasa.gov

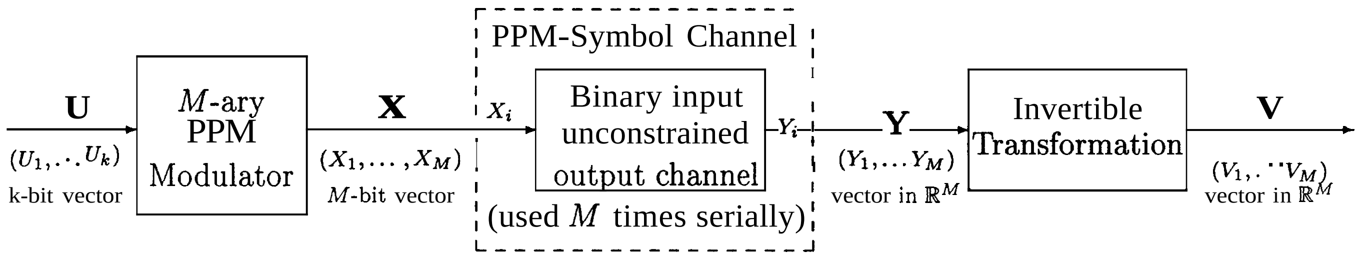

Figure 1. Channel model for PPM signaling.

$\{\mathbf{x}_1,\ldots,\mathbf{x}_M\}$ of a $(2^k,k)$ orthogonal code, where $\mathbf{x}_j$ is a vector of length M containing a one in the jth position. By the symmetry of orthogonal signals, capacity is achieved with an equiprobable distribution on $\mathbf{X}$, i.e., $p(\mathbf{X}=\mathbf{x}_i)=1/M$ for each i, $1\le i\le M$. Thus,

$$C=\int_{\mathbb{R}^M} p(\mathbf{V}=\mathbf{v}|\mathbf{X}=\mathbf{x}_1)\log_2\left[\frac{p(\mathbf{V}=\mathbf{v}|\mathbf{X}=\mathbf{x}_1)}{\frac{1}{M}\sum_{j=1}^{M} p(\mathbf{V}=\mathbf{v}|\mathbf{X}=\mathbf{x}_j)}\right]d\mathbf{v} \text{ bits per channel use.} \tag{1}$$

The elements of $\mathbf{V}$ are independent, and consequently,

$$p(\mathbf{V}=\mathbf{v}|\mathbf{X}=\mathbf{x}_j)=\prod_{i=1}^{M} p(V_i=v_i|\mathbf{X}=\mathbf{x}_j)=p_1(v_j)\prod_{i=1,i\neq j}^{M} p_0(v_i),$$

The bracketed term in Eq. (1) can be expressed as

$$\frac{p(\mathbf{V}=\mathbf{v}|\mathbf{X}=\mathbf{x}_1)}{\frac{1}{M}\sum_{j=1}^{M} p(\mathbf{V}=\mathbf{v}|\mathbf{X}=\mathbf{x}_j)}=\frac{Mp_1(v_1)\prod_{i=1,i\neq 1}^{M} p_0(v_i)}{\sum_{j=1}^{M} p_1(v_j)\prod_{i=1,i\neq j}^{M} p_0(v_i)}=\frac{ML(v_1)}{\sum_{j=1}^{M} L(v_j)},$$

where $L(v)\triangleq p_1(v)/p_0(v)$ is the likelihood ratio of receiving statistic v on the binary-input unconstrained output channel. Thus, the capacity in Eq. (1) can be rewritten in terms of the likelihood ratios of the M slot statistics:

$$\boxed{C=E\log_2\left[\frac{ML(V_1)}{\sum_{j=1}^{M} L(V_j)}\right] \text{ bits per channel use}} \tag{2}$$

where the expectation is taken over $\mathbf{V}$, with V_1 having pdf $p_1(\cdot)$ and V_j having pdf $p_0(\cdot)$, $j>1$. Note that, as expected, Eq. (2) gives a capacity near $\log_2 M$ bits per channel use when the channel is high-quality and the likelihood ratio of V_1 dominates the sum of the other likelihood ratios. Eq. (2) can be numerically evaluated using standard Monte Carlo techniques.

3. CAPACITY FOR SPECIFIC STATISTICAL CHANNEL MODELS

For each statistical channel model below, we define the invertible transformation $\mathbf{Y}\to\mathbf{V}$ in Fig. 1 to normalize the channel and minimize the number of variables. Then we determine $p_0(\cdot)$, $p_1(\cdot)$, and $L(\cdot)$, and plug the expressions into the capacity formula in Eq. (2). Throughout, m_0, m_1 and σ_0^2, σ_1^2 denote the means and variances of Y_j during nonsignal and signal slots, respectively. Two fundamental parameters used in all models are the *SNR parameter* and *excess SNR parameter* we define, respectively, by

$$\rho \triangleq (m_1-m_0)^2/\sigma_0^2 \tag{3}$$
$$\gamma \triangleq (m_1-m_0)^2/(\sigma_1^2-\sigma_0^2). \tag{4}$$

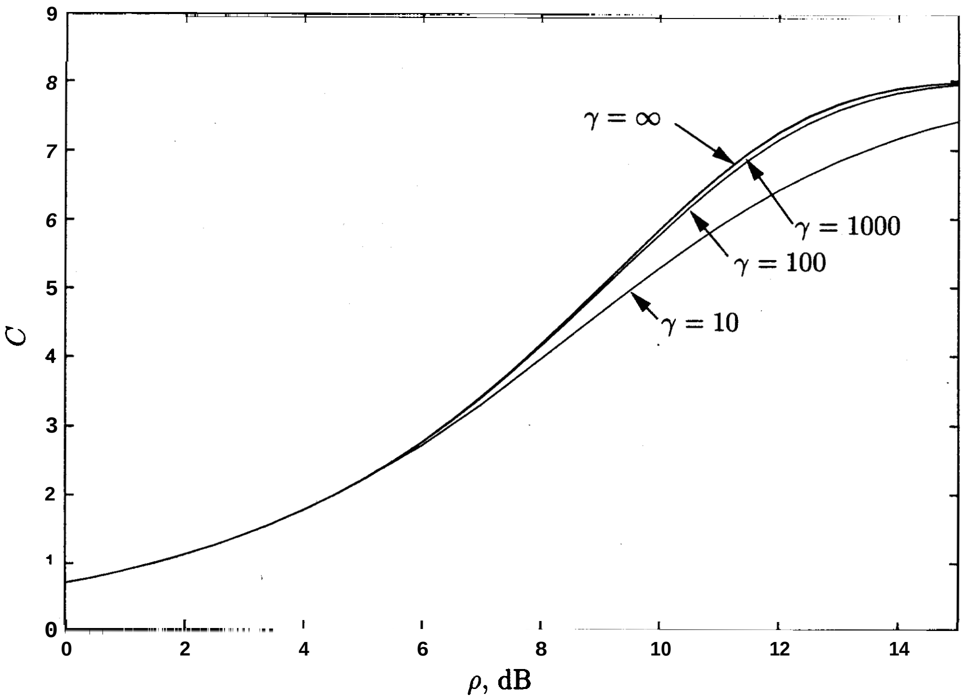

Figure 2. Capacity of **PPM** on **AWGN** channel, versus symbol SNR, **p.**

3.1. AWGN channel model

Despite substantial flaws, the AWGN channel model has been used extensively in the optical communications literature [2–6], and it is the current model used in free-space optical communications link budget software at NASA [7]. The AWGN channel is defined **as** having Gaussian distribution $N(m_1, \sigma_1^2)$ when a one is sent, and $N(m_0, \sigma_0^2)$ when a zero is sent. We let $V_j \triangleq (Y_j - m_0)/\sigma_0$, so that We write these conditional pdfs **as** $\phi((x - m_1)/\sigma_1)/\sigma_1$ and $\phi((x - m_0)/\sigma_0)/\sigma_0$, where $\phi(x) \triangleq \frac{1}{\sqrt{2\pi}} e^{-x^2/2}$. We let $V_j \triangleq (Y_j - m_0)/\sigma_0$, so that

$$\begin{array}{ll} p_1(\cdot), \text{ the pdf of } V_1, \text{ is} & N(\sqrt{\rho}, 1 + \rho/\gamma) \\ p_0(\cdot), \text{ the pdf of } V_j, \text{ is} & N(0,1), \quad j > 1. \end{array}$$

Thus,

$$L(v) = \frac{\gamma}{\rho + \gamma} \exp\left[\frac{-\gamma(v - \sqrt{\rho})}{2(\rho + \gamma)} + \frac{v^2}{2}\right] = \frac{\gamma}{\rho + \gamma} \exp\left[\frac{\rho v^2 + 2\gamma\sqrt{\rho} v - \gamma\rho}{2(\rho + \gamma)}\right].$$

The capacity is given by **Eq.** (2), which becomes

$$C = \log_2 M - E \log_2 \sum_{j=1}^{M} \exp\left[\frac{(V_j - V_1)(\rho(V_j + V_1) + 2\gamma\sqrt{\rho})}{2(\rho + \gamma)}\right] \text{ bits per channel use.} \tag{5}$$

The capacity of **256-PPM** is shown in Fig. **2 as** a function of **p**, for various values of γ. As $\gamma \to \infty$, we have $\sigma_1 \to \sigma_0$, and the signal and noise become independent. That is the usual situation in most RF channels, but distinctly not usual for most optical channels, where the signal and noise are correlated. Nevertheless, in the case when $\sigma_1 = \sigma_0$ (i.e., $\gamma = \infty$), the capacity in **Eq.** (5) simplifies to

$$C = E \log_2 \left[\frac{M}{\sum_{j=1}^{M} e^{\sqrt{\rho}(V_j - V_1)}}\right] \text{ bits per channel use.} \tag{6}$$

The capacity of M-PPM, $M = 2, 4, 8, 16, 32, 64, 128, 256$, is shown in Fig. **3,** when $\sigma_1 = \sigma_0$.

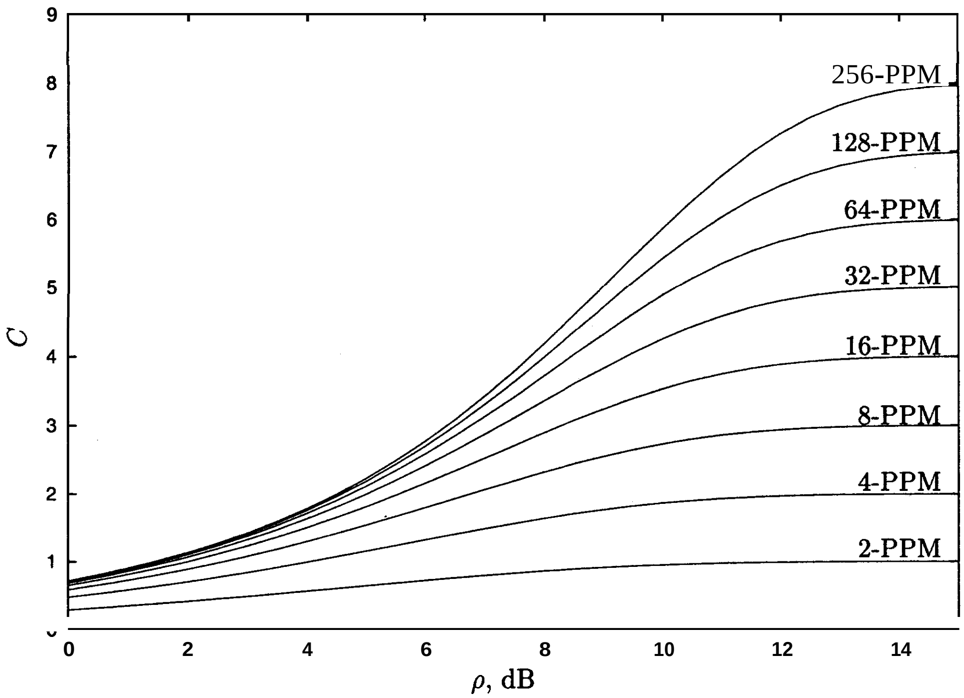

Figure 3. Capacity of PPM on AWGN channel when $\sigma_1 = \sigma_0$, versus symbol SNR, p.

3.2. Webb channel model

A Gaussian model of an Avalanche PhotoDiode (APD) detector output under conditions of negligible background radiation and low APD bulk leakage currents leads to substantial underestimates of optical APD gain and overestimates of system bit error probability [2]. A more accurate approximation of the optical channel statistics governing Y_i has been given by Webb [1]. We write $Y_i \sim W(m, \sigma^2, \delta^2)$ to indicate that $Y_i \triangleq m + oW$, where W is a zero-mean, unit-variance Webb deviate with pdf

$$p_w(w; \delta^2) \triangleq \frac{1}{\sqrt{2\pi}}(1 + w/\delta)^{-3/2} \exp\left[\frac{-w^2}{2(1 + w/\delta)}\right], \quad w > -\delta.$$

The pdf of the unnormalized statistic Y_i, evaluated at y_i, is $p_w((y_i - m)/\sigma; \delta^2)/\sigma$. Unlike the Gaussian distribution, the Webb distribution is not determined solely by its mean and variance; it also depends on the "skewness" parameter 6. Note that as $\delta \to \infty$, the Webb distribution reduces to the normal distribution. See Fig. **4.**

The Webb channel is defined **as** having Webb distribution $W(m_1, \sigma_1^2, \delta_1^2)$ when a one is sent, and $W(m_0, \sigma_0^2, \delta_0^2)$ when a zero is sent, along with the constraint that $\sigma_0^2/\sigma_1^2 = \delta_0^2/\delta_1^2$. As in the AWGN channel, we let $V_j \triangleq (Y_j - m_0)/\sigma_0$, so that

$$\begin{array}{ll} p_1(\cdot), \text{ the pdf of } V_1, \text{ is} & W(\sqrt{\rho}, 1 + \rho/\gamma, (1 + \gamma/\rho)\Delta) \\ p_0(\cdot), \text{ the pdf of } V_j, \text{ is} & W(0, 1, \gamma\Delta/\rho), \quad j > 1, \end{array}$$

A $\triangleq \delta_1^2 - \delta_0^2$. The capacity is given by **Eq.** (2), with

$$L(v) = \frac{p_w\left(\sqrt{\frac{\gamma}{\rho+\gamma}}(v - \sqrt{\rho}); (1 + \gamma/\rho)\Delta\right)}{p_w(v; \gamma\Delta/\rho)}.$$

3.3. Webb Plus Gaussian channel model

Follow-on electronics in a receiver introduce thermal noise to detector outputs. This is accounted for by modeling the system with a Webb plus Gaussian distribution. We denote this by writing $Y_i \sim W(m_0, \sigma_0^2, \delta_0^2) + N(0, \sigma_n^2)$ when

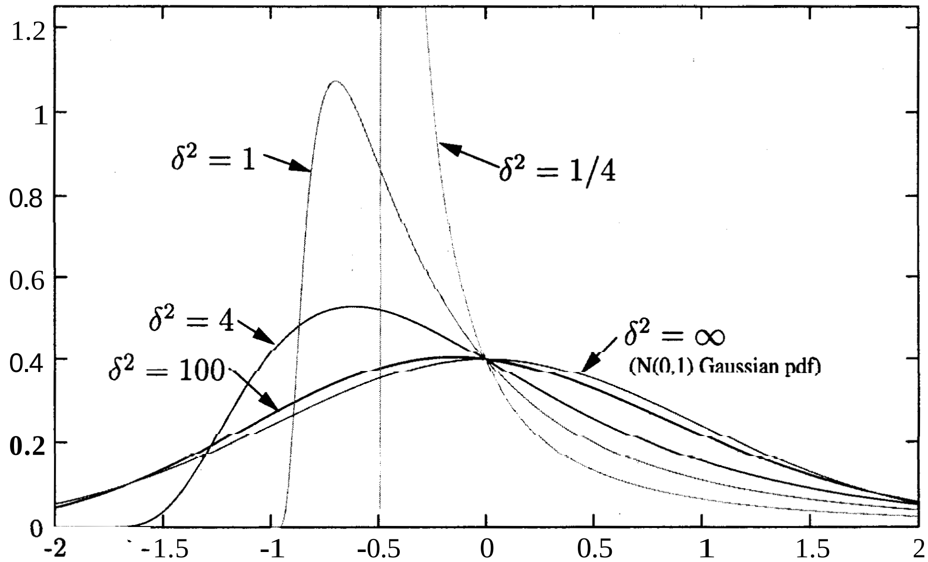

Figure 4. The Standardized Webb pdf, for various δ.

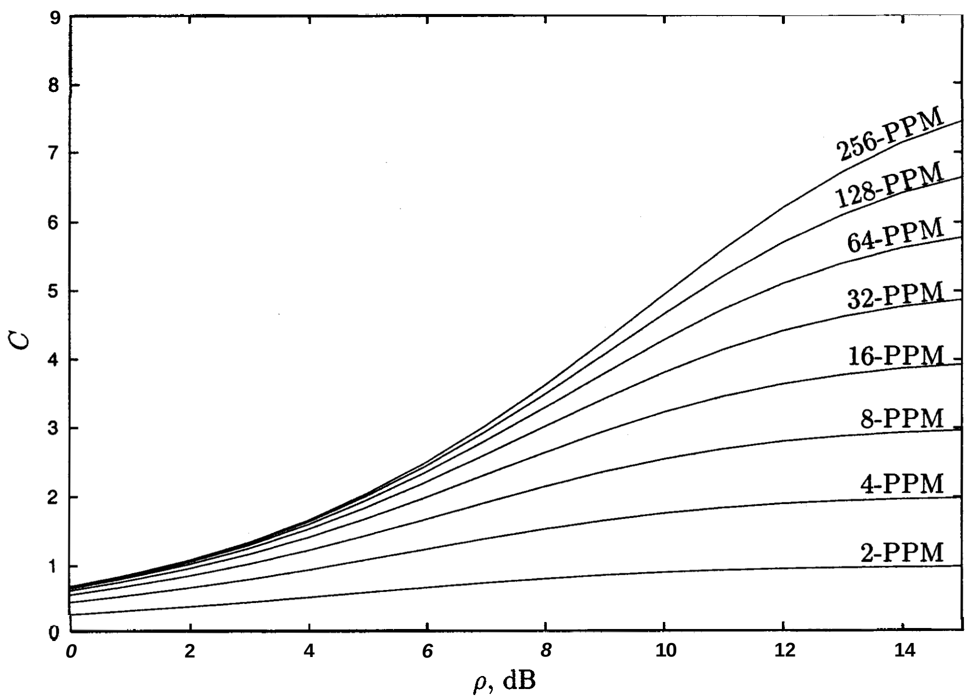

Figure 5. Capacity of PPM on Webb channel) versus symbol SNR, ***p***. γ =?, **A** =?

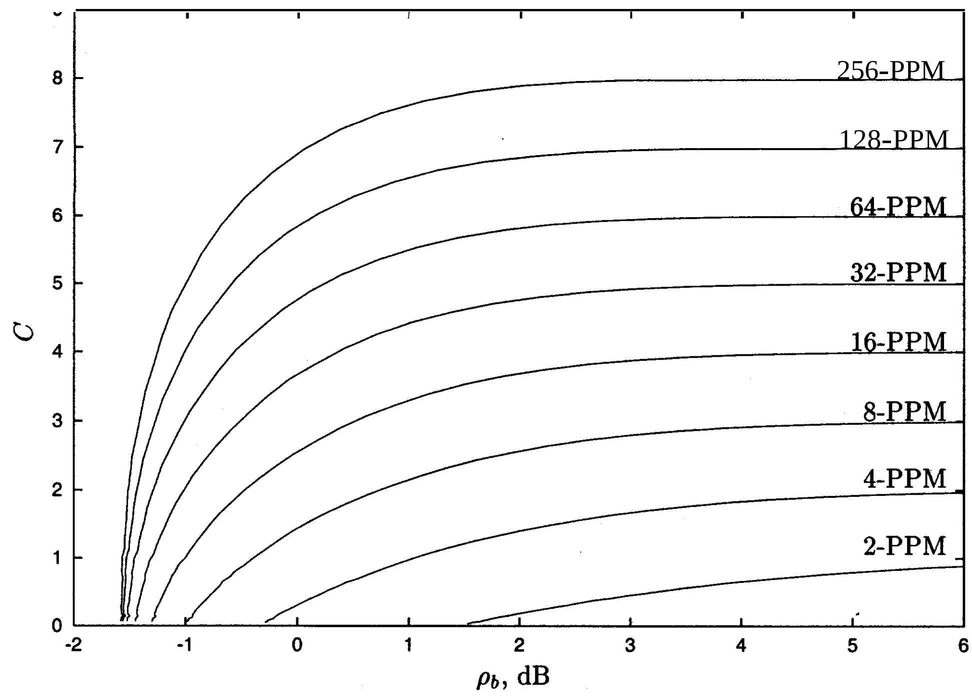

Figure 6. Capacity of PPM on AWGN channel when $\sigma_1 = \sigma_0$, versus bit SNR, ρ_b.

a zero is sent and $Y_i \sim W(m_1, \sigma_1^2, \delta_0^2) + N(0, \sigma_n^2)$ when a one is sent. These conditional pdf's are given by the convolution of the Webb and Gaussian pdf's:

$$p_{wg}(y) = \int_{-\delta_l}^{\infty} \underbrace{\frac{1}{\sigma_n}\phi\left(\frac{y-x}{\sigma_n}\right)}_{\text{AWGN pdf at } y-x} \cdot \underbrace{\frac{1}{\sigma_l}p_w\left(\frac{x-m_l}{\sigma_l}; \delta_l^2\right)}_{\text{Webb pdf at } x} dx, \tag{7}$$

where $l \in \{0,1\}$ indicates the condition that either a 0 or a **1** was sent.

The Webb Plus Gaussian channel is defined **as** having Webb distribution $W(m_1, \sigma_1^2, \delta_1^2) + N(0, \sigma_n^2)$ when a one is sent, and $W(m_0, \sigma_0^2, \delta_0^2) + N(0, \sigma_n^2)$ when a zero is sent, along with the constraint that $\sigma_0^2/\sigma_1^2 = \delta_0^2/\delta_1^2$. We let $V_j \triangleq (Y_j - m_0)/\sigma_0$, so that

$$\begin{aligned} &p_1(\cdot), \text{ the pdf of } V_1, \text{ is} && W(\sqrt{\rho}, 1+\rho/\gamma, (1+\gamma/\rho)\Delta) + N(0,\beta) \\ &p_0(\cdot), \text{ the pdf of } V_j, \text{ is} && W(0, 1, \gamma\Delta/\rho) + N(0,\beta), \quad j > 1, \end{aligned}$$

where A $\triangleq \delta_1^2 - \delta_0^2$, and $\beta \triangleq \sigma_n^2/\sigma_0^2$. The capacity is given by Eq. (2), with

$$L(v) = \frac{\frac{\gamma}{\rho+\gamma}\int_{-(\rho+\gamma)\Delta/\rho}^{\infty} \phi\left(\frac{v-x}{\beta}\right) \cdot p_w\left(\sqrt{\frac{\gamma}{\rho+\gamma}}(x-\sqrt{\rho}); \frac{(\rho+\gamma)\Delta}{\rho}\right) dx}{\int_{-\gamma\Delta/\rho}^{\infty} \phi\left(\frac{v-x}{\beta}\right) \cdot p_w\left(x; \frac{\gamma\Delta}{\rho}\right) dx} \tag{8}$$

4. CAPACITY SENSITIVITY TO PHYSICAL PARAMETERS

An optical link is defined by dozens of physical parameters involving the laser, telescopes, atmosphere, and detector, but these physical parameters affect capacity only in how they affect the values of the three fundamental paramters. The physical parameters we consider are:

- *Laser and Modulator Parameters.* Laser and modulator parameters include the optical frequency ν, the width of the pulse slot T_s, the required deadtime between pulses T_d, the modulation extinction ratio α_{er}, and the order M of the M-ary Pulse Position Modulation (PPM) signal.

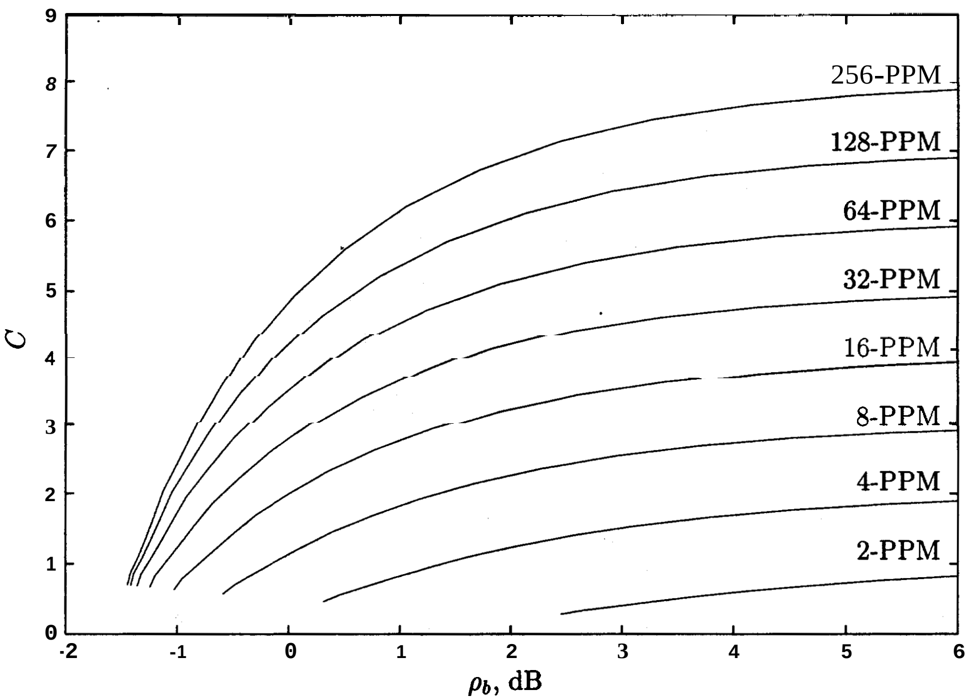

Figure 7. Capacity of PPM on Webb channel, versus bit SNR, ρ_b. γ =?, $\mathbf{A}$ =?

- *Detector Parameters.* Avalanche PhotoDiode (APD) detector parameters include the quantum efficiency η, excess noise factor F, gain G, noise temperature T, load resistance R_L, bulk leakage current I_b, and surface leakage current I_s.
- *Channel Parameters.* Channel parameters include the mean number of background photons incident on the detector $\bar{n}_b$, and the mean number of pulse-induced photons incident on the detector $\bar{n}_s$.

Some other parameters can be expressed in terms of those above, but will not be used explicitly in this article. For example, the ionization ratio k_{eff} is related to F and G by $F = k_{eff}G + (2 - 1/G)(1 - k_{eff})$, the noise equivalent one-sided bandwidth B is set equal to $\frac{1}{2T_s}$, and the optical frequency ν only matters in how it affects $\bar{n}_b$ and $\bar{n}_s$. And for most lasers the modulation extinction ratio has a negligible effect, being on the order of 10^6. Hence, in the remainder of the paper, ν, T_d, and α_{er} will be ignored.

4.1. Relationship of Fundamental and Physical Parameters

The capacity of soft-decision M-ary PPM on the Webb+Gaussian channel is a real-valued function $C(\mathbf{a})$, where $\mathbf{a} = (\rho, \gamma, \mathbf{A}, \beta)$ is the vector of fundamental parameters. The fundamental parameter vector $\mathbf{a}$ can be expressed in terms of physical parameters

$$P = \{\eta, \bar{n}_s, \bar{n}_b, F, I_b, I_s, T_s, T, R_L, G\}$$

by

$$\rho \triangleq \frac{(m_1 - m_0)^2}{\sigma_0^2 + \sigma'^2} = \frac{G^2\eta^2\bar{n}_s^2}{FG^2(\eta\bar{n}_b + \frac{I_bT_s}{e_-}) + \frac{I_sT_s}{e_-} + \frac{2\kappa TT_s}{R_Le_-^2}} \tag{9}$$

$$\gamma \triangleq \frac{(m_1 - m_0)^2}{\sigma_1^2 - \sigma_0^2} = \frac{\eta\bar{n}_s}{F} \tag{10}$$

$$\Delta \triangleq \delta_1^2 - \delta_0^2 = \frac{\eta\bar{n}_sF}{(F-1)^2} \tag{11}$$

$$\beta \triangleq \frac{\sigma_n^2}{\sigma_0^2} = \frac{\frac{I_sT_s}{e_-} + \frac{2\kappa TT_s}{R_Le_-^2}}{FG^2(\eta\bar{n}_b + \frac{I_bT_s}{e_-})} \tag{12}$$

Expressions of parameters m_0, m $\sim\sigma_0^2$, σ_1^2, σ_n^2, d d; in terms of of the physical parameters can be found in, e.g., [2,8–10].

4.2. Capacity Sensitivity

The sensitivity of capacity to a fundamental or physical parameter x at operating point **a** is defined as the partial derivative of the logarithm of capacity with respect to the logarithm of the parameter:

$$\text{Capacity sensitivity with respect to x} \triangleq \frac{\partial \log C(\mathbf{a})}{\text{dlogx}}.$$

The logarithm is used to emphasize the sensitivity of the parameter *without regard to the units in which the parameter is measured,* and it allows us to effectively compare the relative sensitivities of various parameters. This is in contrast to the linear partial derivative $\frac{\partial C}{\partial x}$, which has one value when, for example, x $= T_s$ is measured in nanoseconds, and a value one billion times smaller when $X = T_s$ is measured in seconds. If x is a physical parameter, we may express the sensitivity with respect to x at operating point **a** as

$$\frac{\partial \log C(\mathbf{a})}{\partial \log x} = \left(\frac{1}{C(\mathbf{a})}\right)\frac{\partial C(\mathbf{a})}{\partial \log x} = \left(\frac{x}{C(\mathbf{a})}\right)\frac{\partial C(\mathbf{a})}{\partial x} = \left(\frac{x}{C(\mathbf{a})}\right)\nabla C(\mathbf{a})\cdot\frac{\partial \mathbf{a}}{\partial x}, \tag{13}$$

i.e., the normalized dot product of the gradient of $C(\mathbf{a})$ and the vector $\frac{\partial \mathbf{a}}{\partial x}$ which forms one of the columns of the Jacobian matrix of a:

$$J(\mathbf{a}) = \begin{bmatrix} \frac{\partial\rho}{\partial\eta} & \frac{\partial\rho}{\partial\bar{n}_s} & \frac{\partial\rho}{\partial\bar{n}_b} & \frac{\partial\rho}{\partial F} & \frac{\partial\rho}{\partial I_b} & \frac{\partial\rho}{\partial I_s} & \frac{\partial\rho}{\partial T_s} & \frac{\partial\rho}{\partial T} & \frac{\partial\rho}{\partial R_L} & \frac{\partial\rho}{\partial G} \\ \frac{\partial\gamma}{\partial\eta} & \frac{\partial\gamma}{\partial\bar{n}_s} & \frac{\partial\gamma}{\partial\bar{n}_b} & \frac{\partial\gamma}{\partial F} & \frac{\partial\gamma}{\partial I_b} & \frac{\partial\gamma}{\partial I_s} & \frac{\partial\gamma}{\partial T_s} & \frac{\partial\gamma}{\partial T} & \frac{\partial\gamma}{\partial R_L} & \frac{\partial\gamma}{\partial G} \\ \frac{\partial\Delta}{\partial\eta} & \frac{\partial\Delta}{\partial\bar{n}_s} & \frac{\partial\Delta}{\partial\bar{n}_b} & \frac{\partial\Delta}{\partial F} & \frac{\partial\Delta}{\partial I_b} & \frac{\partial\Delta}{\partial I_s} & \frac{\partial\Delta}{\partial T_s} & \frac{\partial\Delta}{\partial T} & \frac{\partial\Delta}{\partial R_L} & \frac{\partial\Delta}{\partial G} \\ \frac{\partial\beta}{\partial\eta} & \frac{\partial\beta}{\partial\bar{n}_s} & \frac{\partial\beta}{\partial\bar{n}_b} & \frac{\partial\beta}{\partial F} & \frac{\partial\beta}{\partial I_b} & \frac{\partial\beta}{\partial I_s} & \frac{\partial\beta}{\partial T_s} & \frac{\partial\beta}{\partial T} & \frac{\partial\beta}{\partial R_L} & \frac{\partial\beta}{\partial G} \end{bmatrix}$$

To determine the sensitivity of capacity with respect to one of the physical parameters, we need only determine the gradient of the capacity expressed as a function of the four fundamental parameters and form the inner product with the appropriate column of $J(\mathbf{a})$.

4.3. Numerical Results

As an example of this calculation, we consider a Webb plus Gaussian channel model, a strong signal, strong background, and optimized APD gain. We use an EG&G SliK APD detector with physical parameters $\eta = 0.38$, F $= 2.42572$, $I_b = 40$fA, $I,$ $= 2.00$nA, $T = 300$K, and $R_L = 179.7\text{k}\Omega$. It has been shown [11,12] that for this set of parameters, G = 65 is the optimum gain for hard-decision detection of 256-PPM. This is also a good estimate of the gain which maximizes capacity on the soft-decision channel, which turned out to be G = 59. We use a Q-switched Nd:YAG laser modulated with a slot width of $T_s = 31.25$ns. A high signal strength $\bar{n}_s = 100$ is incident on the detector, and a high background level $\bar{n}_b = 100$ is also present, which corresponds to reception on a clear, sunny day.

Plugging these parameters into Eq.s (9-12), it follows that $\rho = 13.7$, $\gamma = 15.7$, $\mathbf{A} = 45.3$, and $\beta = 0.145$. For computational complexity reasons, the likelihood function $L(v)$ for these parameters was precomputed, and is shown in Fig. 8. Using the finite differences method, the partial derivative of capacity with respect to each fundamental parameter, i.e., the components of the gradient, were computed. These components, when normalized as in **Eq.** (13), give the capacity sensitivity with respect to each of the fundamental parameters, which is shown in Fig. 9. Note that by far, the SNR parameter ρ has the greatest effect on capacity, followed by the excess SNR parameter γ. The blending fraction β and skewness difference **A** play a lesser role.

The Jacobian was evaluated and used to determine the $\frac{\partial C}{\partial x}$ for each physical parameter x. The capacity sensitivity with respect to the physical parameters is shown in Fig. 10.

5. CONCLUSIONS

We have derived a general formula for the capacity of PPM on a memoryless, soft output channel. This formula was evaluated for specific channel models: Gaussian, Webb, and Webb plus Gaussian. In this process, we have distilled the multitude of parameters that describe these channels to two, three, and four fundamental parameters,

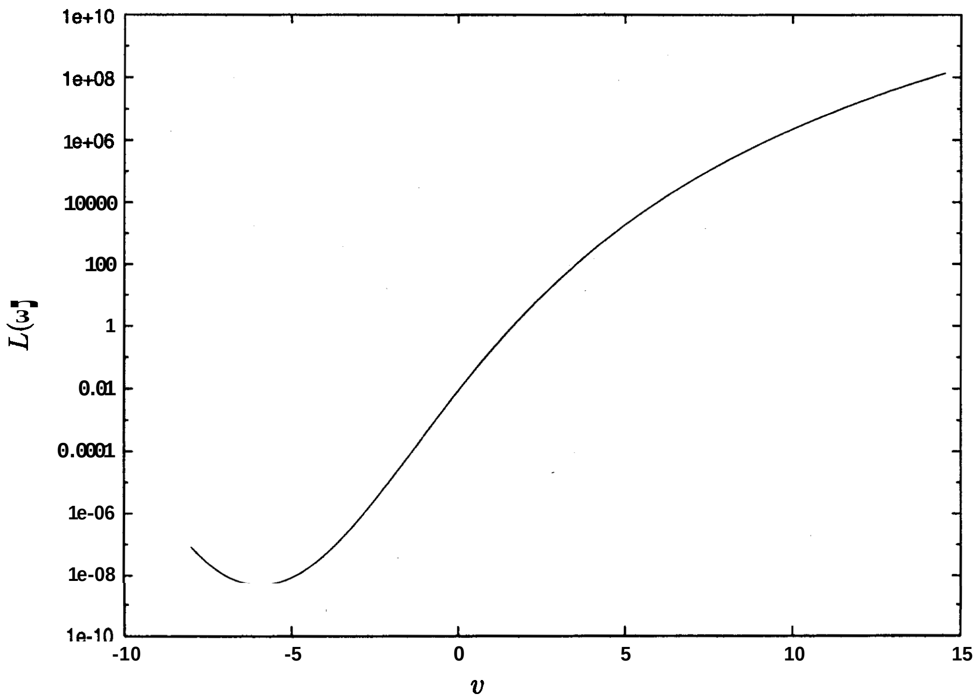

Figure 8. Likelihood function $L(v)$ over the range stored in the look-up table.

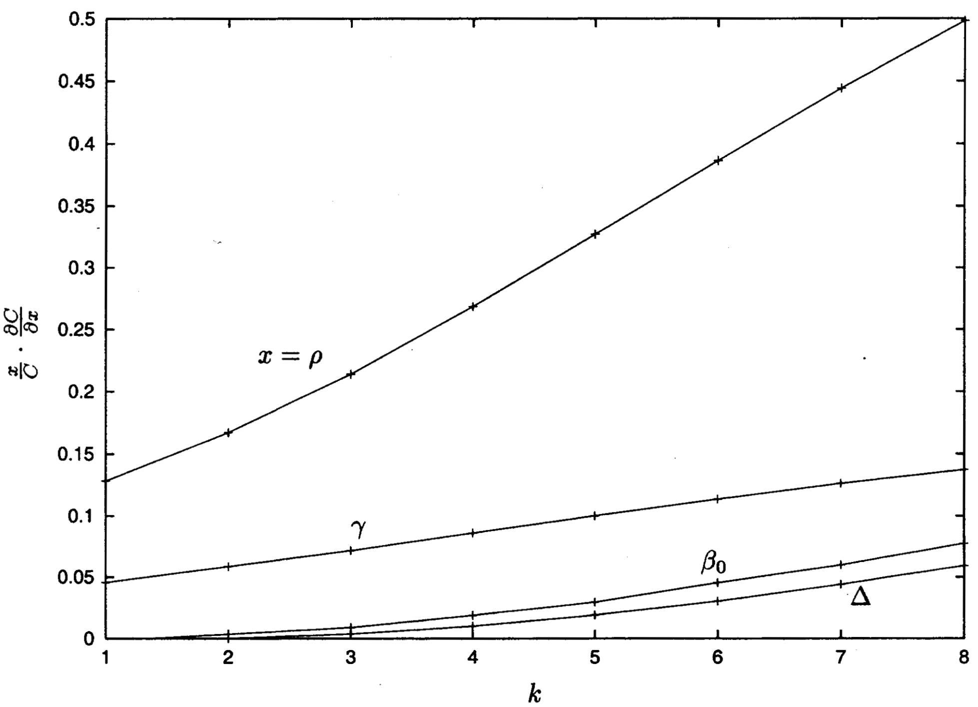

Figure 9. Capacity sensitivity of 2^k-PPM, with respect to fundamental parameters.

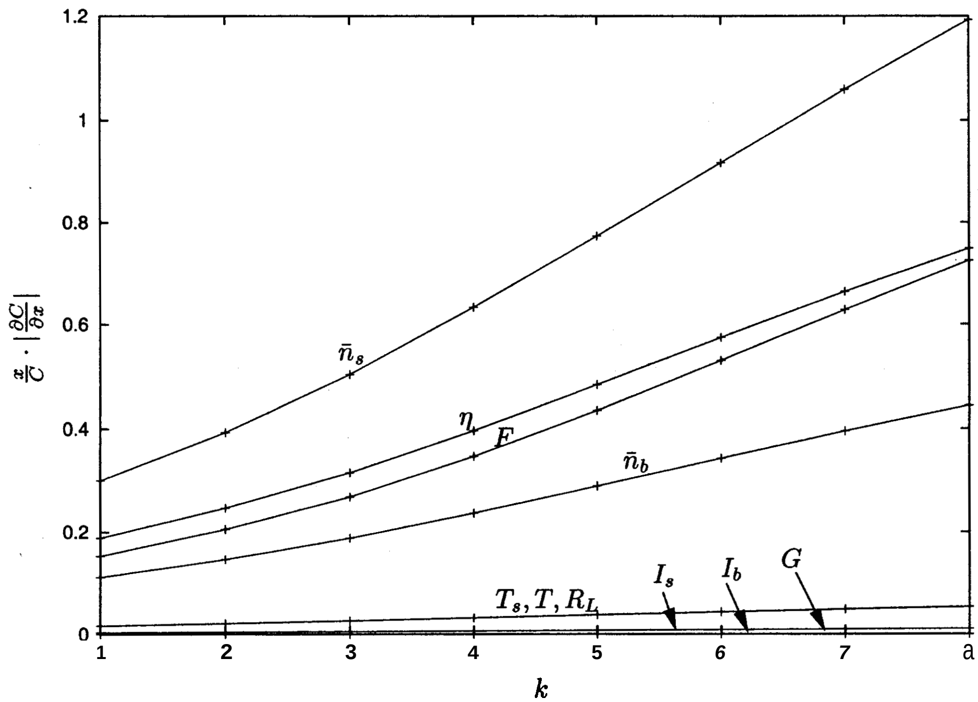

Figure 10. Capacity sensitivity of 2^k-PPM with respect to physical parameters.

respectively. The capacity of the optical channel expressed a function of bit-SNR is similar to what we see on the RF channel, with a brick-wall limit at **-1.59** dB.

In conjunction with a Jacobian matrix that describes the relationship between four fundamental parameters and ten physical parameters, we determined the sensitivity of the capacity with respect to any of the four fundamental parameters and any single physical parameter.

The capacity was found to be most sensitive to the primary SNR parameter ρ, with the other three fundamental parameters playing lesser roles. The overall relative importance of the physical parameters, with respect to capacity sensitivity, was found to be fairly consistent. The physical parameters, in order of influence, are: the signal intensity, the quantum efficiency, the excess noise factor, the background intensity, the gain, the slot width, the equivalent noise temperature, the load resistance, the surface leakage current, and the bulk leakage current.

REFERENCES

1. P. P. Webb, R. J. McIntyre, and J. Conradi, "Properties of avalanche photodiodes," *RCA Review* **35,** pp. 234–**278,** June **1974.**
2. F. M. Davidson and **X.** Sun, "Gaussian approximation versus nearly exact performance analysis of optical communication systems with PPM signaling and APD receivers," *IEEE Trans. Commun.* **36,** pp. **1185–1192,** Nov. **1988.**
3. D. Divsalar, R. M. Gagliardi, and J. H. Yuen, "PPM performance for Reed-Solomon decoding over an optical-RF relay link," *IEEE Trans. Commun.* **COM-32,** pp. **302–305,** Mar. **1984.**
4. **L.** W. Hughes, **"A** simple upper bound on the error probability for orthogonal signals in white noise," *IEEE Trans. Commun.* **40,** p. **670,** Apr. **1992.**
5. G. S. Mecherle, *Maximized data rate capability for optical communication using semiconductor devices with pulse position modulation.* PhD thesis, University of Southern California, May **1986.**
6. V. Vilnrotter, "Optical receivers using rough reflectors,'' JPL publication **25,** JPL, May **1985.**
7. M. Jeganathan and S. Mecherle, *A technical manual for FOCAS **2.0** – Free-space Optical Communications Analysis Software*, May **1998.**

8. J. T. K. Tang and K. B. Letaief, "The use of WMC distribution for performance evaluation of APD optical communication systems," *IEEE Trans. Commun.* **46,** pp. 279–285, Feb. 1998.
9. S. Dolinar, D. Divsalar, J. Hamkins, and F. Pollara, "Capacity of PPM on Gaussian and Webb channels," *TMO Progress Report* , Aug. 2000.
10. J. Hamkins, **S.** Dolinar, and D. Divsalar, "Optical channel capacity sensitivity," *TMO Progress Report* , Nov. 2000.
11. M. Srinivasan and V. Vilnrotter, "Symbol-error probabilities for pulse-position modulation signaling with an avalanche photodiode receiver and Gaussian thermal noise,'' *TMO Progress Report* **42-134,** pp. **1–11,** Aug. 1998.
12. J. Hamkins, "The capacity of APD-detected PPM," *TMO Progress Report* **42,** pp. 1–19, Aug. 1999.